Deuteron Spin-Lattice Relaxation Times in Undercooled Aqueous Potassium- and Cesium Halide Solutions

W. Fink, H. Radkowitsch, and E. W. Lang

Institut für Biophysik und physikalische Biochemie, Universität Regensburg, Regensburg

Aqueous emulsions of potassium- and cesium halides in cycloalkane mixtures can be undercooled at a pressure of 225 MPa to temperatures around 170 K. In these emulsions deuterium spin-lattice relaxation times T_1 have been determined as function of salt concentration, temperature and pressure at magnetic fields of 2.4 Tesla and 7.0 Tesla. The frequency and temperature dependence of the relaxation time curves is described quantitatively within a motional model which is consistent with known local structural features in these solutions. Model parameters deduced are compared with those obtained in related studies of the other alkali-halides, and conclusions are drawn regarding the influence of structure and composition on molecular motions.

Introduction

Deuteron (^{2}H) spin-lattice relaxation time T_1 measurements monitor reorientational motions of water molecules (D_2O) rather directly. Application of the emulsion technique [1] to aqueous electrolyte solutions allows the relaxation times over the entire concentration range to be followed into the undercooled metastable phase down to the homogeneous nucleation temperature T_H [2–6]. The latter shifts to lower temperatures with increasing salt concentration and also with increasing pressure as is shown in Figure 1. Aqueous solutions can be undercooled quite substantially. At high solute concentrations nucleation may even become kinetically impossible, and the solutions freeze into an amorphous solid at the glass transition [7].

On reducing the temperature, the molecular motions of the hydrogen bonded network slow down to a time scale comparable with the Larmour period $2\pi/\omega$ of the deuterium nucleus. Whereas at high temperatures only average correlation times can be obtained, details of the molecular motions can be deduced from the form of the relaxation time curve at low temperatures. This has been demonstrated for aqueous LiCl [3, 8, 9], $MgCl_2$ [4], NaCl and NaJ [5] solutions. Consistent with the average local structure in ionic solutions [10, 11] a motional model has been developed which could account for the most promi-

nent features of the relaxation time curves for all solute concentrations up to saturation.

The present study extends these investigations to the potassium- and cesium halides dissolved in heavy water. We report deuteron spin-lattice relaxation times $T_1(^2$H$)$ in aqueous $KX (X = Cl: c \leq 3.7 \, m$, Br: $c \leq 4.6 \, m$, $J: c = 3 \, m$) and $CsX (X = CL: c \leq 9 \, m$, Br: $c \leq 3 \, m$) solutions for temperatures $283 \, K \geq T \geq 170 \, K$ and at pressures up to $p = 225 \, MPa$. The primary interest is devoted to the high pressure isobars from which the relevant model parameters can be deduced. These allow a detailed comparison of characteristics of molecular motions of water molecules in the undercooled aqueous alkali-halide solutions studied so far.

Experiment

To prevent heterogeneous nucleation upon cooling all salt solutions had to be prepared as emulsions [1, 12]. Prior to use, all salts have been dried under vacuum and stored over P_2O_5 on a vacuum line for 48 h. The solutions were prepared from a stock solution of the anhydrous salt (Merck, Darmstadt, FRG) and triply distilled D_2O (99.75%, Merck, Darmstadt). Emulsions were prepared by mixing equal amounts of the salt solution with a mixture of methylcyclohexane (24 wt%), methylcyclopentane (24 wt%) and the surfactant sorbitanetristearate (Span 65, 2 wt%). Before mixing, all components had to be degassed by at least five freeze-pump-thaw cycles to remove dissolved oxy-
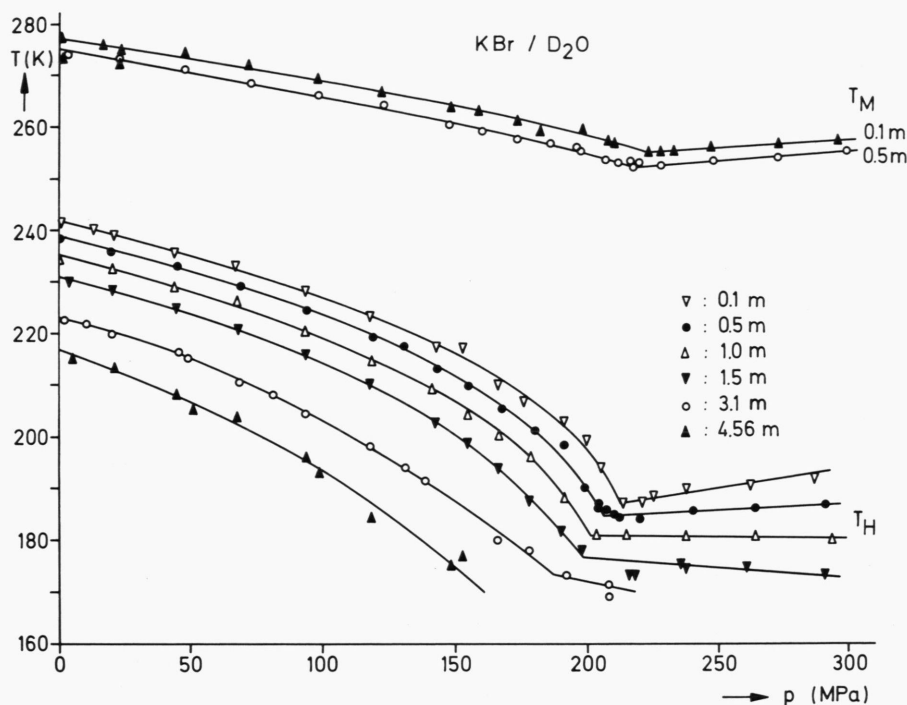

Fig. 1. Pressure and concentration dependence of the homogeneous necluation temperature T_H of the system KBr/D_2O. Upper curves give the melting pressure curve T_m for two concentrations.

gen. The mixing was done in a glove bag under an argon atmosphere by pressing the mixture through a stainless steel net within a syringe. Finally, the emulsion had to be filled into strengthened glass cells [13]. All T_1 experiments were performed with the inversion recovery pulse sequence (Freeman-Hill modification) on a Varian XL-100 spectrometer at 15.35 MHz or on a Bruker MSL 300 multi-purpose solid-liquid spectrometer at 46.07 MHz. The relaxation times are considered reliable to $\pm 10\%$. The temperatures have been measured with a miniature chromel-alumel thermocouple (Philips, Kassel, FRG) and are accurate to ± 1 K. The pressure has been measured with a precission Bourdon gauge (Heise, Connecticut, USA) to ± 0.5 MPa.

Theory

NMR relaxation rate measurements, when applied to deuterium (^{2}H) nuclei, monitor single molecule reorientation rather directly. The information is contained in the spectral density function $g(\omega)$, which is the Fourier-Laplace transform of the reorientational auto-correlation function $G(t)$ of the water molecules [14]. At ambient temperatures this function decays

rapidly on the NMR time scale rendering T_1 insensitive to the shape of $g(\omega)$. The relaxation rate is then simply proportional to an average correlation time $\tau_{av} \approx \int G(t)\, dt$, thus any details of $G(t)$ are washed out. At low temperatures the reorientation of the water molecules in the undercooled solutions is slowed down sufficiently for the relaxation rate to become sensitive to the functional form of the spectral density $g(\omega)$. But because $g(\omega)$ cannot be obtained over a large frequency range with NMR methods, motional models are still necessary to deduce a form of the orientational correlation function consistent with the experimental data sampled at different frequencies.

Motional Model for the Hydration Water

A quantitative discussion of the dynamics of water molecules in aqueous electrolyte solutions will therefor be given in terms of a motional model developed recently to deduce a spectral density $g(\omega)$ for water molecules adjacent to ionic solutes which is consistent with the average local structures in these systems. The model decomposes the orientational fluctuations of the water molecules into small amplitude librations about their mean orientation. These fast torsional oscillations are superimposed onto anisotropic fluctua-

tions around the local director (ion-oxygen distance in the case of hydrated cations) with correlation time τ_i. It may be expected from electrostatic considerations that fluctuations around the director are less strongly hindered than fluctuations around any perpendicular axis. Hence, to keep the model simple with a minimum of adjustable parameters, only these least hindered fluctuations are taken into account. In addition to these local modes there is an isotropic tumbling of the molecules around the ion with correlation time τ_r. Also chemical exchange [15] between hydration sites and bulk sites must be accounted for because of short mean residence times τ_{ex} of water molecules adjacent to the cations.

Hydration Water Relaxation Rate

The model yields the following expression for the deuteron relaxation rate R_1 of the hydration water [3–5, 8]:

$$(R_1)_{hyd} = (3\pi^2/20)\,((\chi_{eff})^2/\omega_0)\,((1/4)\,(3\cos^2\beta_{DF} - 1)^2$$
$$\cdot F(\omega_0\tau_0) + 3\sin^2\beta_{DF}\cos^2\beta_{DF}\cdot F(\omega_0\tau_1)$$
$$+ (3/4)\sin^4\beta_{DF}\cdot F(\omega_0\tau_2))$$

with

$$F(\omega\tau) = 2\cdot g(\omega\tau) + 8\cdot g(2\omega\tau), \tag{2}$$

$$g(m\omega\tau) = \omega\tau/(1 + (m\omega\tau)^2), \tag{3}$$

and

$$1/\tau_0 = 1/\tau_r + 1/\tau_{ex}, \tag{4a}$$
$$1/\tau_1 = 1/\tau_0 + 1/\tau_i, \tag{4b}$$
$$1/\tau_2 = 1/\tau_0 + 4/\tau_i. \tag{4c}$$

The slower modes of motion provide the main contribution to $g(\omega)$, whereas the effect of the fast torsional oscillations can be incorporated into an effective, librationally averaged quadrupole coupling constant [8, 16]

$$\chi_{eff} = (\sum|\langle D^2_{02}(\Omega_{FI})\rangle|^2)^{1/2}\cdot\chi$$
$$\simeq (1/2)\,(3\langle\cos^2\beta_{FI}\rangle - 1)\cdot\chi, \tag{5}$$

β_{FI} is the angle between the z-axis of the instantaneous principal frame of the electric field gradient tensor (I) and the equilibrium orientation of the OD-bond (F) in the quasi-static local configuration. β_{DF} relates this equilibrium orientation of the OD-bond to the local director frame (D).

The above expressions imply that time-scale separation pertains between the torsional and the diffusive

modes, that the anisotropic diffusive mode and the isotropic tumbling mode are statistically independent, that the mean residence time τ_{ex} is at least of the order of the correlation times, and that the interaction is completely randomized on exchange [15].

Two-Site Approximation

Because the exchange between hydration sites and bulk sites is fast ($T_1 > \tau_{ex}$), an average relaxation time can be observed only. It will be calculated within a two-state approximation [3] as a mole-fraction weighted average according to

$$R_1(T, p, R) = (n_h/R)\,(R_1)_{hyd} + ((R - n_h)/R)(R_1)_{bulk} \tag{6}$$

with n_h the dynamic hydration number of the cations and $R\,(= \text{moles }D_2O/\text{mole salt})$ the water/salt ratio.

Results

Effects of Pressure and Ionic Solutes

The isothermal pressure dependence of the deuterium spin-lattice relaxation times $T_1\,(^2H)$ is illustrated in Figs. 2 and 3 for various potassium- and cesium halide solutions and for two temperatures corresponding to the stable and the metastable, undercooled phase. In the undercooled phase T_1 increases upon compression, the effect being most pronounced at low temperatures and low solute concentrations. Hence the anomalous increase in rotational mobility with increasing pressure [17] decreases with increasing concentration of ionic solutes. Figures 2 and 3 demonstrate also that in these systems T_1 is always longer than in neat undercooled D_2O. Again the difference $T_1(T, p, c) - T_1(T, p, c = 0)$ is largest at low pressure, is always positive and increases with increasing concentration. This is qualitatively different from the aqueous solutions of LiCl [2, 3, 8, 9], $MgCl_2$ [2, 4], NaCl and NaJ [2, 5] studied so far. Increasing the anionic radius tends to diminish the anomalous pressure effect further. This anion effect is again most pronounced at low pressures.

Relaxation Rates in the Dispersion Regime

Figures 4–6 show the high pressure ($p = 225\,MPa$) isobars for all systems and all concentrations studied. They extend to the lowest temperatures that could be
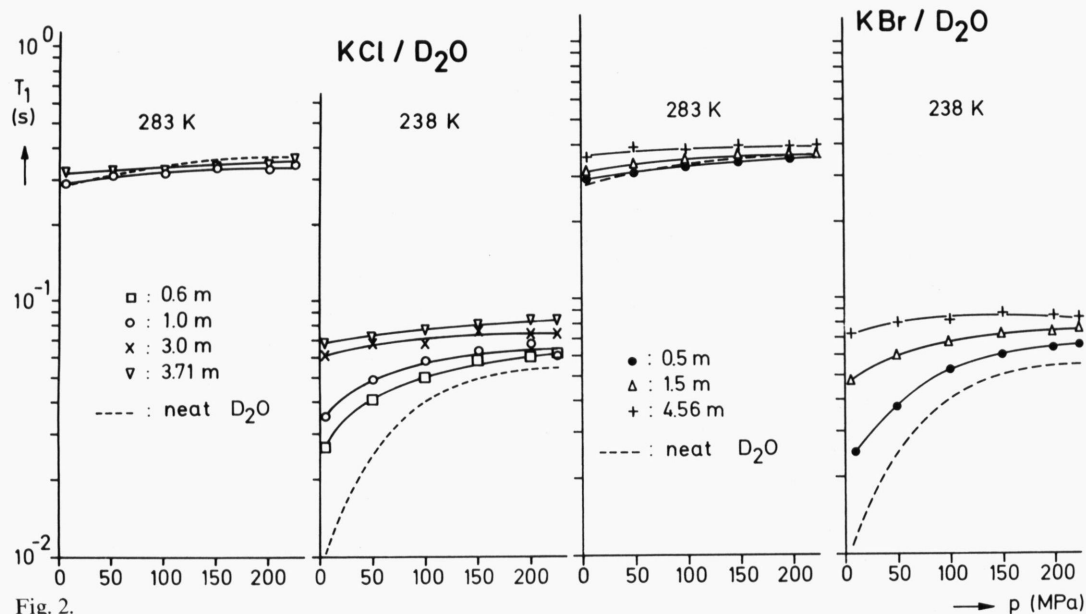
KCl / D$_2$O
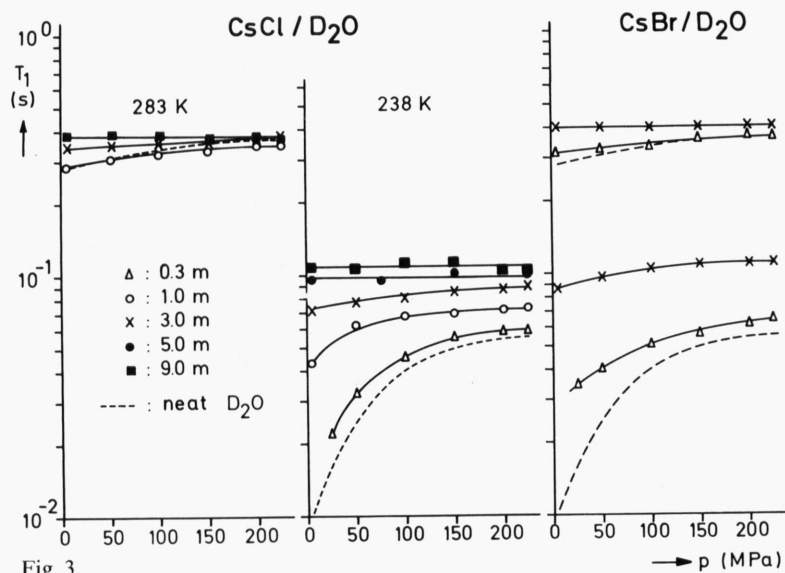
283 K 238 K

T_1 (s)

□ : 0.6 m
○ : 1.0 m
× : 3.0 m
▽ : 3.71 m
--- : neat D$_2$O

Fig. 2.

KBr / D$_2$O

283 K 238 K

● : 0.5 m
△ : 1.5 m
+ : 4.56 m
--- : neat D$_2$O

p (MPa)

CsCl / D$_2$O

283 K 238 K

T_1 (s)

△ : 0.3 m
○ : 1.0 m
× : 3.0 m
● : 5.0 m
■ : 9.0 m
--- : neat D$_2$O

CsBr / D$_2$O

Fig. 3.

p (MPa)

^{2}H-T_1 in KCl/D$_2$O and KJ/D$_2$O

T_1 (s)

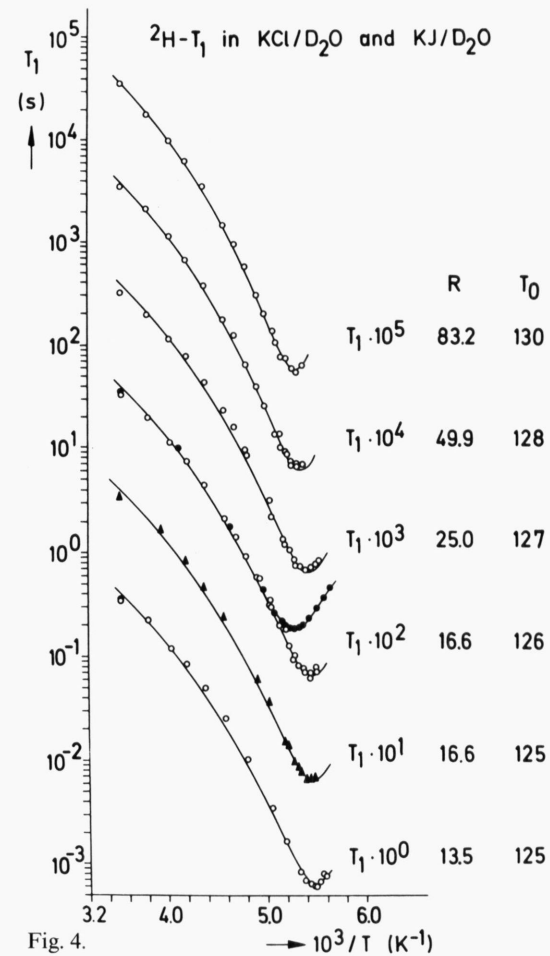|	R	T_0
$T_1 \cdot 10^5$	83.2	130
$T_1 \cdot 10^4$	49.9	128
$T_1 \cdot 10^3$	25.0	127
$T_1 \cdot 10^2$	16.6	126
$T_1 \cdot 10^1$	16.6	125
$T_1 \cdot 10^0$	13.5	125

Fig. 4.

$10^3/T$ (K^{-1})

Fig. 2. Comparison of the pressure and concentration dependence of T_1-isotherms in the solutions KX/D$_2$O (X = Cl, Br).

Fig. 3. Comparison of the pressure and concentration dependence of T_1-isotherms in the solutions CsX (X = Cl, Br).

Fig. 4. Isobaric temperature dependence of $T_1(T)$ in the system KCl/D$_2$O for all compositions investigated (R = moles D$_2$O/mole salt). Full curves correspond to (1) and (6). $p = 225$ MPa.
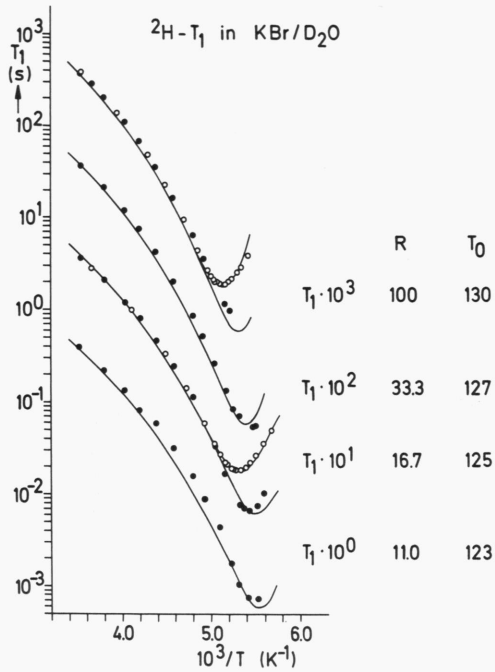
Fig. 5. Isobaric temperature dependence of $T_1(T)$ in the system KBr/D$_2$O for all compositions investigated. Full curves correspond to (1) and (6). $p = 225$ MPa.
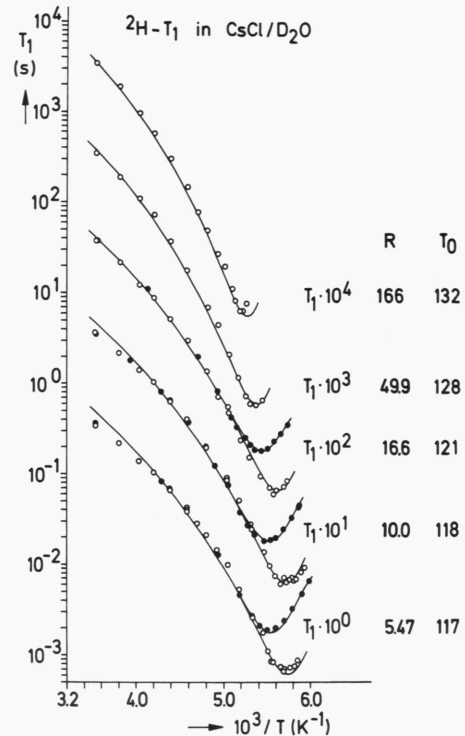

Fig. 6. Isobaric temperature dependence of $T_1(T)$ in the system CsCl/D$_2$O for all compositions investigated. Full curves correspond to (1) and (6). $p = 225$ MPa.

obtained. At still lower temperatures the lines become very broad, characteristic of a solid.

All isobars exhibit a minimum corresponding to a maximal spin-lattice relaxation rate. In some cases the relaxation time curves could be measured at two fields, $B_0 = 2.35$ Tesla and $B_0 = 7.0$ Tesla corresponding to Larmour frequences of $\omega_0/2\pi = 15.35$ MHz and 46.07 MHz. At temperatures near and below the T_1 minimum the spin-lattice interaction fluctuates at a rate comparable with the Larmour period, hence the $T_1(T)$ curves become frequency dependent. The high field measurements are especially valuable because more data in the slow motion regime ($T < T_{\min}(\omega)$) could be sampled.

A characteristic feature of all isobars is their strong non-Arrhenius temperature dependence typical for most undercooled liquids displaying slow relaxations [18, 19]. It is interesting that the curvature of the $T_1(T, p = 225$ MPa) isobars is practically identical in all solutions studied, including those investigated previously, and that it is identical to the one observed in neat undercooled D$_2$O. Another interesting observation concerns the composition dependence of the temperature $T_{\min}$ of the T_1-minimum, which is compiled in

Tables 1 and 2. $T_{\min}$ decreases with increasing concentration of ionic solutes in the potassium- and cesium halide solutions, whereas it increased in the lithium-, magnesium- and sodium halide solutions studied hitherto. It is tempting to relate this observation to the structure breaking and structure making capabilities of the solutes.

Discussion

Estimation and Interpretation of the Model Parameters

Orientation of Hydration Water

In recent investigations we studied the influence of Li$^+$, Mg^{2+} and Na$^+$ upon molecular motions of water molecules in undercooled aqueous solutions under hydrostatic pressure [2–6, 8, 9]. The cations in these solutions are generally considered to exert an appreciable influence upon adjacent water molecules. They

Table 1. Compilation of minimum temperatures T_{min} of the relaxation time curves $T_1(T, p = 225\,\mathrm{MPa})$ and related ideal glass temperatures [a) $\omega/2\pi = 15.35\,\mathrm{MHz}$, b) $46.07\,\mathrm{MHz}$].

		KCl					KBr				KJ	CsCl				
c		0.6	1.0	2.0	3.0	3.7	0.5	1.5	3.0	4.6	3.0	0.3	1.0	3.0	5.0	9.0
R		83.2	50.0	25.0	16.7	13.5	100.0	33.3	16.7	11.0	16.7	167.0	50.0	16.7	10.0	5.6
T_{min}	a)	189	187	186	185	184		186	184	182	184	192	187	178	175	175
	b)				189		195		189					185	184	182
T_0		130	128	127	126	125	130	127	125	123	125	132	128	121	118	117

Table 2. Comparison of model parameters entering (1) to (6) for all alkali-halide solutions studied hitherto [a) X = Cl, Br, J, b) X = Cl, Br].

	LiCl	NaCl	NaJ	KCl, KBr, KJ	CsCl, CsBr
$\tau_{00} \pm 20$ (fs)	200	120	85	65	65
τ_{i0} (fs)	80	62	69	62	62
$E_a \pm 0.8$ (kJ/mol)	19.8	18.7	18.7	17.9	17.0
B_r (kJ/mol)	5.7	5.7	5.7	5.7	5.7
$\chi \pm 10$ (kHz)	192	192	201.1	201.1	201.1
$n_h \pm 1$	$R = 4.55$ 4.55 $R \geq 6.25$ 6	$R = 9.5$ 5 $R \geq 2.5$ 6	$R = 4.2$ 3 $R = 8.6$ 4 $R \geq 16.7$ 6	$R \geq 13.5^a$ 7 $R \geq 11.0^b$ 6	$R = 5.6$ 2 $R = 10$ 5 $R \geq 16.7$ 8

R (moles D_2O/mol salt), a) KCl, b) KBr, KJ.

induce a well-defined average local structure within the coordination sphere for time spans at least comparable to the correlation times characterizing orientational and positional flucutations of water molecules hydrating the cations [20–22]. Furthermore, these fluctuations are slowed down in the neighbourhood of the cations [22]. Because of their smaller charge density, the halide anions (except for the F^--anion) impose much weaker structural and motional constraints upon water molecules, which can be neglected in most respects.

The presently studied systems represent borderline case concerning size and charge density of the cations compared with the anions. Still we will assume that the cations K^+ and Cs^+ are the more favorably hydrated species, i.e. they are considered to exert the stronger influence upon the structure and dynamics of the water molecules in the solutions because of their slightly stronger interactions with water molecules [11, 23, 24].

Although ion-water interactions decrease with increasing ionic radius, water molecules are still preferentially oriented beneath K^+ or Cs^+ with their hydrogen atoms pointing away from the cations [11, 23, 25]. Hence the latter must induce at least some anisotropy of orientational fluctuations of water molecules also. In most salt hydrates [26] the water molecules around the cations possess a tetragonal orientation, i.e. their dipole moment vector is tilted away from the local director by 54 deg., roughly. Hence β_{DF} has been calculated accordingly, although a range of tilt angles and ion-oxygen distances is certainly encountered with these weakly hydrating cations [25, 27]. However, β_{DF} does not change much in going from a tetragonal to a trigonal orientation, rendering the $^2H\text{-}T_1$ fairly insensitive to the average orientation of the water molecules in the hydration shell [9]. Also the $^2H\text{-}T_1$ do not depend on the ion-oxygen distance.

The Coupling Constant χ

The librationally averaged quadrupole coupling constant χ_{eff} can be determined from the relaxation rate maximum. Contrary to the more strongly hydrat-
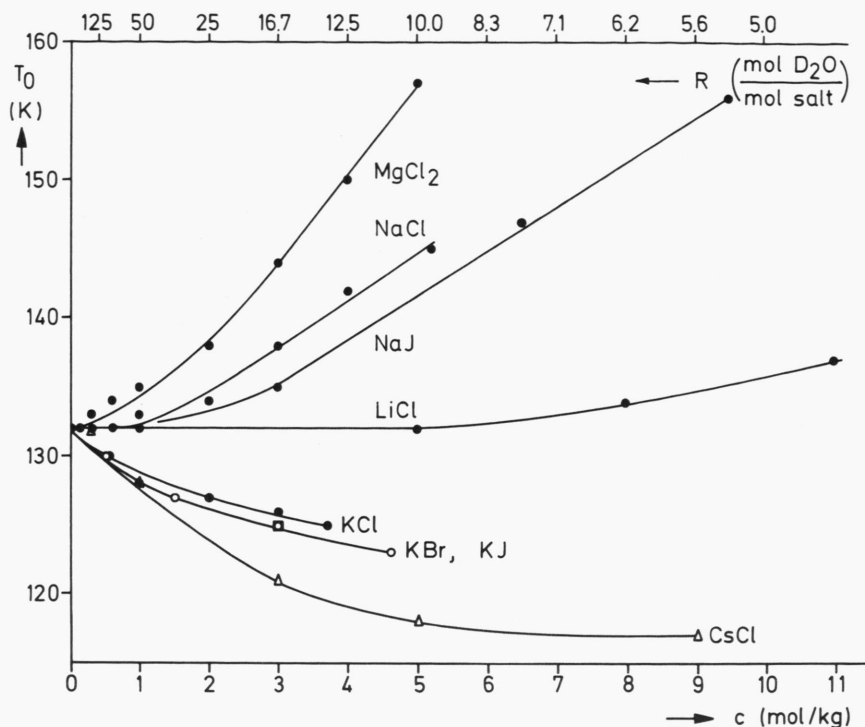
Fig. 7. Comparison of concentration dependence of ideal glass temperatures T_0 for all undercooled electrolyte solutions studied hetherto (Ref. [3–5, 9].

ing cations, χ_{eff} turned out to be unaffected by Cs^+ and K^+ cations compared to its value in pure water.

Temperature Dependence of Tumbling and Exchange Modes

The most prominent feature of the relaxation time curves is the strongly non-Arrhenius temperature dependence, which has also been observed in neat undercooled water [16, 17]. This led to the suggestion that the temperature dependence of the global tumbling motions in the solutions, like the α-process in glass-forming systems, may be represented by a Vogel-Tammann-Fulcher (VTF) law [12, 18, 19] according to

$$\tau_0 = \tau_{00} \cdot \exp \{B_r/(T - T_0(R, p))\}, \qquad (7)$$

as has been found appropriate in many undercooled liquids.

T_0 is an ideal glass transition temperature signifying a kinetic localization phenomenon, where global motional modes become arrested on macroscopic time scales. $T_0(R)$ can be predicted according to an empirical correlation between $T_{min}(R)$ and experimental glass transition temperatures $T_g(R)$, as has been demonstrated recently [2–6]. As experimental glass

transition temperatures are almost lacking for the systems studied here [7], we will assume that a correlation between $T_{min}(R)$ and $T_0(R)$ exists for all alkali-halide solutions.

The interesting new feature is that in the solutions with strongly hydrating cations T_{min}, and consequently T_0, shifts to higher temperatures with increasing solute concentration whereas in the current systems with weakly hydrating cations T_{min}, hence T_0, decreases upon the addition of ionic solutes.

Figure 7 further reveals a strong dependence of T_0 on the cationic radius and a weak dependence on the anionic radius. In general, T_0 decreases with increasing ion size, the only exception being Li^+, as was observed with experimental glass temperatures also [28].

The cations K^+ and Cs^+ are often said to exhibit negative hydrations (structure breaking) [22]. This is in accord with our finding that T_1, hence the average molecular mobility ($1/\tau_{av}$), is always (i.e. for all p and T) larger in potassium and cesium halide solutions than it is in neat water (see Figures 2, 3). If τ_{av} follows a VTF-type behaviour essentially, then an enhanced average mobility upon addition of ionic solutes is tantamount to saying that T_0 is reduced with

increasing solute concentration. In consequence, the solution must be cooled to a lower temperature before molecular motions become arrested.

The preexponential factor τ_{00} in (7) can be estimated from T_1-data at high temperatures, where the relaxation time curve is dominated by tumbling and exchange processes. Varying τ_{00} changes the relaxation time curve at high temperatures most and leaves it virtually unchanged in the dispersion region ($T \leq T_{\min}$).

Temperature Dependence
of the Local Anisotropic Mode

In systems with strongly hydrating cations the relaxation rate did not slow down in the slow motion regime ($T < T_{\min}$) as strongly as expected according to a VTF-type behaviour [2–6]. Rather, the $T_1(T)$ curves show a changeover to an approximate Arrhenius behaviour at low temperatures [8, 9]. It resembles the splitting off of a secondary relaxation process (β-process) in glass-forming systems. This feature is explained in the current motional model in terms of thermally activated local anisotropic modes with a concomittant Arrhenius temperature dependence according to

$$\tau_i = \tau_{i0} \cdot \exp(E_a/kT). \qquad (8)$$

τ_{i0} must be related to an attempt frequency for barrier crossing, hence corresponds to the inverse of an average librational frequency of the primary hydration water component [29] and has been calculated accordingly.

Because of the weaker temperatures dependence, these anisotropic fluctuations become the faster modes at low temperatures and provide the more efficient relaxation channels, hence dominate the relaxation. The return to an Arrhenius dependence leads to a characteristic asymmetry of the relaxation time curve around the minimum, which is the more pronounced the larger the polarizing power of the respective cations is. Note that because of (6) these features are most clearly seen in those cases where high concentrations ($R \simeq n_h$) can be reached [3–6].

But the cations in this study impose only weak geometrical constraints upon orientational fluctuations. Consequently we expect less clear indications of these anisotropic modes in the relaxation time curves. Also, because of their larger surface area, reorientations of the water molecules around the local director
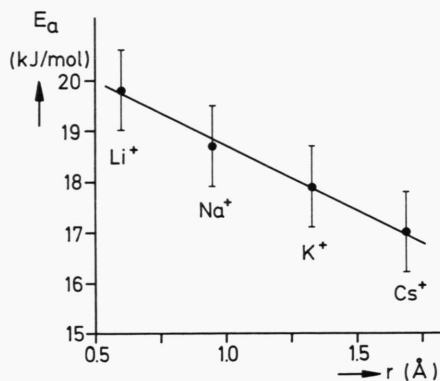

Fig. 8. Comparison of average rotational barriers E_a in (7) hindering reorientations around the local director within the hydration shell of the various cations as deduced according to the current motional model.

should be less hindered. This is corroborated by the finding that the apparent activation energy E_a decreases, giving shorter τ_i, with increasing ion size (see Figure 8).

Because the local anisotropic mode does not contribute to the relaxation in the fast motion regime significantly, the rotational barriers can only be deduced from the high field measurements which extend well into the slow motion regime.

Calculation of the Relaxation Rates

The model parameters χ_{eff} and τ_{00} have been estimated from high field data of the 3 m KCl solutions for the potassium halides and the 3 m CsCl solutions for the cesium halide solutions. The rotational barrier E_a has then been determined by a least squares fit with (6).

Of course, both rates in (6) have to be evaluated at the same reduced temperature $T - T_0(R)$ appropriate to the solution under investigation, because the clusters of hydrated cations are in dynamic equilibrium with bulk water molecules. The influence of the anions upon the bulk water dynamics is simply incorporated into the proper glass temperature T_0 of the solutions.

Table 2 compiles all model parameters related to the hydration water dynamics of K$^+$ and Cs$^+$ according to (1). With these parameters and a properly choosen $T_0(R)$ the relaxation time curves $T_1(T, R)$ can be calculated with (6) for all solutions of composition R.

Composition Dependence of the Hydration Number

At high concentrations, the hydration number n_h had to be adjusted to reach good overall agreement. It turned out to be strongly concentration dependent and to become smaller than the coordination numbers n_c (K^+: 7–8, Cs^+: 8) deduced from computer simulations [11, 25]. Applying (6) to a given solution, n_h was set equal to the coordination number n_c in a first attempt and then reduced until good overall agreement with the data has been reached. The shape of the relaxation time curve is fairly sensitive to the value of n_h as well as to the rotational barrier E_a for $T \leq T_{min}$. In fact, lowering n_h or enhancing E_a influences the relaxation time curve in nearly the same way in this temperature range. Reducing n_h enlarges the number of water molecules in the system which display bulk water dynamics. Hence a smaller hydration number n_h

leads to deeper and less broad T_1-minima. Also the curvature of the relaxation time curve becomes more pronounced in an Arrhenius plot because the influence of the anisotropic fluctuations displaying Arrhenius behaviour is reduced thereby. The reduction of the hydration number is most pronounced in the CsCl solutions. This is in accord with the common believe [30] that large single charged ions lack specific hydration characteristics according to most criteria.

[1] D. H. Rassmussen and A. P. McKenzie in H. H. Jellinek ed. 'Water Structure and the Water-Polymer Interface', Plenum Press, New York 1972.
[2] E. W. Lang, W. Fink, and H.-D. Lüdemann, J. Physique **45**, C7-173 (1984).
[3] E. W. Lang and H.-D. Lüdemann, Ber. Bunsenges. Phys. Chem. **89**, 508 (1985).
[4] W. Fink and E. W. Lang, J. Phys. Chem. (1988) in press.
[5] W. Fink, H. Radkowitsch, and E. W. Lang, Chem. Phys. (1988) in press.
[6] E. W. Lang, H. Radkowitsch, and W. Fink, Proc. XIth AIRAPT Conference, Kiew 1987, in press.
[7] H. Kanno and C. A. Angell, J. Phys. Chem. **81**, 2639 (1977).
[8] E. W. Lang and L. Piculell in G. W. Neilson, J. E. Enderby eds. 'Water and Aqueous Solutions', Hilger, Bristol 1986.
[9] E. W. Lang and F. X. Prielmeier, Ber. Bunsenges. Phys. Chem. (1988), in press.
[10] J. E. Enderby, Ann. Rev. Phys. Chem. **34**, 155 (1983).
[11] K. Heinzinger, Physica **131 B**, 196 (1985).
[12] C. A. Angell in F. Frands ed., 'Water – A Comprehensive Treatise', Vol. 7 Plenum Press, New York 1982.
[13] E. W. Lang, R. Rauchschwalbe, and H.-D. Lüdemann, High Temperatures – High Pressures **9**, 519 (1977).
[14] H. W. Spieß in P. Diehl, E. Fluck, R. Kosfeld eds., NMR – Basic Principles and Progress, Vol. 15 Springer Verlag, Berlin 1978.
[15] H. Wennerström, Mol. Phys. **24**, 69 (1972).
[16] E. W. Lang, L. Piculell, and H.-K. Lüdemann, J. Chem. Phys. **81**, 3820 (1984).

[17] E. W. Lang and H.-K. Lüdemann, Angew. Chem. Int. Engl. **21**, 315 (1982).
[18] J. Jäckle, Rep. Prog. Phys. **49**, 171 (1986).
[19] R. G. Palmer in J. L. van Hemmen, I. Morgenstern eds., 'Heidelberg Colloquium on Glassy Dynamics', Lecture Notes in Physics, Vol. 275, Springer, Berlin 1987.
[20] R. W. Impey, P. A. Madden, and I. R. McDonald, J. Phys. Chem. **87**, 5071 (1983).
[21] H. Friedman, Chemica Scripta **25**, 42 (1985).
[22] H. G. Hertz in F. Franks ed., 'Water – A comprehensive Treatise', Vol. 3, Plenum Press, New York 1973.
[23] M. Migliore, S. L. Fornili, E. Spohr, G. Palinkas, and K. Heinzinger, Z. Naturforsch. **41 a**, 826 (1986).
[24] M. Migliore, S. L. Fornili, E. Spohr, and K. Heinzinger, Z. Naturforsch. **42 a**, 227 (1987).
[25] K. Heinzinger and G. Palinkas in H. Kleeberg ed., 'Interactions of Water in Ionic and Nonionic Hydrates', Springer Verlag, Berlin 1987.
[26] H. L. Friedman and L. Lewis, J. Solut. Chem. **5**, 445 (1976).
[27] G. Heinje, W. A. P. Luck, and K. Heinzinger, J. Phys. Chem. **91**, 331 (1987).
[28] H. Kanno, I. Shirotani, and Sh. Minomura, Bull. Chem. Soc. Japan **54**, 2607 (1981).
[29] D. W. James and R. F. Armishaw, Aust. J. Chem. **28**, 1179 (1975).
[30] B. E. Conway, 'Ionic Hydration in Chemistry and Biophysics', Elsevier, Amsterdam 1981.